10-15-2019

Direct and indirect measurements of the magnetic and magnetocaloric properties of Ni0.895Cr0.105MnGe1.05 melt-spun ribbons in high magnetic fields

Anil Aryal
Southern Illinois University Carbondale

Yuri Koshkid'ko
Wlodzimierz Trzebiatowski Institute of Low Temperature and Structure Research of the Polish Academy of Sciences

Igor Dubenko
Southern Illinois University Carbondale

C. F. Sánchez-Valdés
Universidad Autónoma de Ciudad Juárez

J. L. Sánchez Llamazares
Instituto Potosino de Investigacion Cientifica y Tecnologica

See next page for additional authors

Recommended Citation

Aryal, A., Koshkid'ko, Y., Dubenko, I., Sánchez-Valdés, C., Sánchez Llamazares, J., Lähderanta, E., Pandey, S., Granovsky, A., Cwik, J., Stadler, S., & Ali, N. (2019). Direct and indirect measurements of the magnetic and magnetocaloric properties of Ni0.895Cr0.105MnGe1.05 melt-spun ribbons in high magnetic fields. *Journal of Magnetism and Magnetic Materials, 488* https://doi.org/10.1016/j.jmmm.2019.165359

Journal of Magnetism and Magnetic Materials 488 (2019) 165359

Contents lists available at ScienceDirect

Journal of Magnetism and Magnetic Materials

journal homepage: www.elsevier.com/locate/jmmm

Research articles

Direct and indirect measurements of the magnetic and magnetocaloric properties of $Ni_{0.895}Cr_{0.105}MnGe_{1.05}$ melt-spun ribbons in high magnetic fields

Anil Aryal[a,*], Yuri Koshkid'ko[b], Igor Dubenko[a], C.F. Sánchez-Valdés[c], J.L. Sánchez Llamazares[d,*], E. Lähderanta[e], Sudip Pandey[a], Alexander Granovsky[f], Jacek Cwik[b], Shane Stadler[g], Naushad Ali[a]

[a] Department of Physics, Southern Illinois University, Carbondale, IL 62901 USA
[b] Institute of Low Temperature and Structure Research, PAS, 50-950 Wroclaw, Poland
[c] División Multidisciplinaria, Ciudad Universitaria, Universidad Autónoma de Ciudad Juárez (UACJ), calle José de Jesús Macías Delgado # 18100, Ciudad Juárez 32579, Chihuahua, Mexico
[d] Instituto Potosino de Investigación Científica y Tecnológica A.C., Camino a la Presa San José 2055, Col. Lomas 4ª, San Luis Potosí, S.L.P. 78216, Mexico
[e] Lappeenranta University of Technology, 53851, Finland
[f] Faculty of Physics, Lomonosov Moscow State University, Moscow 119991, Russia
[g] Department of Physics & Astronomy, Louisiana State University, Baton Rouge, LA 70803 USA

ARTICLE INFO

Keywords:
Ni-Cr-Mn-Ge melt-spun ribbons
Phase transitions
Adiabatic temperature change
Magnetocaloric effect

ABSTRACT

We report the magnetic and magnetocaloric properties of rapidly solidified $Ni_{0.895}Cr_{0.105}MnGe_{1.05}$ melt-spun ribbons studied by both direct (adiabatic temperature change) and indirect (isothermal magnetic entropy change) methods in intermediate and high magnetic fields up to 10 T. The maximum values of the adiabatic temperature changes (ΔT_{ad}) and magnetic entropy changes ($|\Delta S_M|$) were found to be ~2.6 K ($\mu_o H$ = 10 T) and 4.4 J kg^{-1} K^{-1} ($\mu_o \Delta H$ = 5 T), respectively, near the Curie temperature (T_C). The ΔT_{ad} curves and magnetization isotherms were found to be completely reversible, which indicates the high degree of reversibility of the MCEs in this system. A large temperature span (of about 61 K) and a non-saturating behavior of ΔT_{ad} were observed at magnetic fields up to 10 T. The adiabatic temperature change was found to be a linear function of $(\mu_o H)^{2/3}$ near T_C, in accordance with the Landau theory of phase transitions.

1. Introduction

The magnetocaloric effect (MCE) is a magneto-thermal property of any ferromagnetic (FM) material that is characterized by the thermal dependency of both the isothermal magnetic entropy change (ΔS_M) and the adiabatic temperature change (ΔT_{ad}) in response to the change in an external magnetic field $\mu_o H$. Both physical quantities show their maximum absolute values, $|\Delta S_M^{peak}|$ and ΔT_{ad}^{max}, near the Curie temperature (T_C). However, several material families such as Gd-Si-Ge, La-Fe-Si, Mn-Fe-P, Mn-As-Sb, and Ni-Mn-(In,Ga,Sn) Heusler alloys undergo giant first-order magnetostructural transitions (MSTs) associated with coupled magnetic and structural transitions, resulting in large MCEs [1–6]. The large MCEs displayed by these materials have attracted attention in the last two decades due to their potential application in magnetic refrigeration, an emerging solid-state cooling technology that is environmentally friendly and energy efficient compared to traditional refrigeration [7,8].

Recently, alloys derived from the stoichiometric 1:1:1 MnNiGe and MnCoGe compounds, belonging to the MnTX (T = 3*d* transition elements and X = Ge, Si) material family have been actively studied since they exhibit large MCEs associated with a change in crystal structure from a high temperature austenite to a low temperature martensite structure. The crystal structure of the high temperature austenite phase is hexagonal (Ni_2In-type, space group $P6_3/mmc$) and the low temperature martensite phase is orthorhombic (TiNiSi-type, space group *Pnma*). In stoichiometric NiMnGe and MnCoGe alloys, the martensitic transitions take place at temperatures T_t = 470 K and 650 K, far above the magnetic transitions at the Neel (T_N = 346 K) and Curie (T_C ~334 K) temperatures, respectively [9,10]. A coincidence of the magnetic and structural transitions, i.e., the magnetostructural transitions, resulting in giant and tunable MCEs in terms of $|\Delta S_M^{peak}|$, have already been reported in these systems by changes in stoichiometry, adding interstitial atoms, doping, application of external pressure, and isostructural alloying [see, for instance, 11–19 and Refs. therein].

* Corresponding authors.
E-mail addresses: aryalanil@siu.edu (A. Aryal), jose.sanchez@ipicyt.edu.mx (J.L. Sánchez Llamazares).

https://doi.org/10.1016/j.jmmm.2019.165359
Received 13 February 2019; Received in revised form 24 April 2019; Accepted 22 May 2019
Available online 23 May 2019
0304-8853/

It is well known that the MCE can be characterized by two important parameters, ΔS_M and ΔT_{ad}. Both quantities are equally important to evaluate the performance of a magnetocaloric material for refrigeration purposes. For applications, not only large ΔS_M^{peak} values but also a large ΔT_{ad}^{max} is desired since it acts as a driving force for heat transfer from the cold to the hot reservoirs during a refrigeration cycle. Reports [11–19 and Refs. therein] show that the MCE in NiMnGe and MnCoGe based alloys have extensively been studied through indirect measurements, i.e., by experimentally determining $\Delta S_M(T)$ from a set of isothermal magnetization $M(\mu_o H)$ curves measured through the phase transition. Large $|\Delta S_M^{peak}|$ values up to 37.8 J kg^{-1} K^{-1} (for $\mu_o\Delta H$ = 2 T at 192 K), 53.3 J kg^{-1} K^{-1} (for $\mu_o\Delta H$ = 5 T at 321 K), and 47.3 J kg^{-1} K^{-1} (for $\mu_o\Delta H$ = 5 T at 287 K) have been reported for (Mn,Fe)NiGe, (Mn,Cu)CoGe, and $MnCoGeB_{0.02}$ alloys, respectively [20–22]. However, reports on the direct measurements, i.e., $\Delta T_{ad}(T)$, a more reliable and straightforward measurement, in these systems are scarce [22–24].

In this work we present the experimental results on the MCE properties of $Ni_{0.895}Cr_{0.105}MnGe_{1.05}$ ribbons using both indirect and direct methods with a focus on the latter. The current study provides an opportunity to understand the magnetic and MCE properties of this system at high magnetic fields up to 10 T.

2. Experiment

Melt-spun ribbon flakes of nominal composition $Ni_{0.895}Cr_{0.105}MnGe_{1.05}$ were fabricated from a bulk polycrystalline arc-melted ingot under a high purity argon atmosphere with a linear speed of the rotating copper wheel of 25 ms^{-1} using an Edmund Bühler model SC melt spinner system [12]. From scanning electron microscopy (SEM) images it was determined that the as-solidified ribbons obtained had an average thickness of 15 ± 1 μm. The phase purities and crystal structures were determined by room temperature X-ray diffraction (XRD) measurements using CuKα radiation. The magnetization measurements were performed using a superconducting quantum interference device (SQUID by Quantum Design) magnetometer in the temperature interval 5–400 K in applied magnetic fields up to 5 T. The thermal protocols used to measure the isofield $M(T)$ and isothermal $M(\mu_o H)$ curves are as follows: for $M(T)$ curves, the samples were first cooled to 10 K from 400 K at zero field. The zero-field-cooling (ZFC) measurements were taken while heating the samples to 400 K in an applied magnetic field, and then followed by a field-cooled-cooling (FCC) measurement to 10 K, and then a field-cooled-heating (FCH) measurement from 10 K to 400 K. For the $M(\mu_o H)$ curves, a "backward and forward" heating-cooling protocol was used. This thermal protocol prevents an over estimation of the peak value of ΔS_M and ensures an accurate temperature location of the peak of the $\Delta S_M(T)$ curve [25]. A home-built apparatus was used to directly measure $\Delta T_{ad}(T)$. Details about the device design, construction, and development are given in Ref. [26]. The direct measurement of ΔT_{ad} was carried out using the "sample extraction method" in fields up to 10 T and in a temperature range of 100–250 K [26]. To improve the thermal contact between the ribbons and the thermocouple, the ribbons were placed in a capsule that had a small hole on one side. The thermocouple was inserted through the hole and into the capsule. The powder in the capsule was then pressed in with a screw, which was threaded into the base of the capsule to ensure good thermal contact between the sample and thermocouple.

3. Results and discussion

Fig. 1 shows the indexed room temperature XRD pattern of $Ni_{0.895}Cr_{0.105}MnGe_{1.05}$ ribbon flakes. Analysis of the XRD pattern revealed that the as-quenched ribbons crystallize into a single-phase with the Ni_2In-type hexagonal structure. The calculated values of the lattice parameters a and c of the hexagonal structure at room temperature were found to be 4.086(1) Å and 5.392(1) Å, respectively, with c/a ratio ~1.32. The degree of hexagonal distortion in this compound calculated using $(1 - c/a) \times 100\%$ was found to be ~32%. The obtained structure, value of the lattice parameters, and c/a ratio are in good agreement with those previously reported for the hexagonal NiMnGe compounds [9,11].

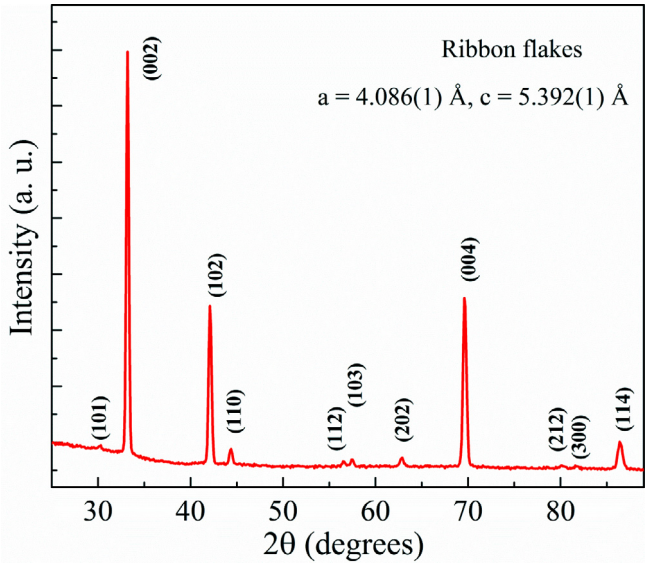

Fig. 1. Room temperature X-ray diffraction pattern of $Ni_{0.895}Cr_{0.105}MnGe_{1.05}$ ribbon flakes. The XRD peak indexing is based on the hexagonal Ni_2In-type crystal structure. The Miller indices are shown in brackets.

For polycrystalline NiMnGe–based compounds with a Ni_2In–type hexagonal structure, the peak intensities of the strongest lines corresponding to (1 0 2), (1 1 0), and (2 0 2) planes are 100%, 100%, and 50%, respectively [27]. In the case of ribbons, the intensities of the major peaks (1 0 2), (1 1 0), and (2 0 2) relative to (0 0 2) peak with the highest intensity was found to be 43%, 11%, and 9%, respectively, indicating the presence of crystallographic texture along the (*0 0 l*) direction. The ribbons' texture was further verified by SEM images, which exhibited columnar-grain microstructures with its axis oriented perpendicular to the ribbon surface. The SEM images and discussion of microstructures of $Ni_{0.895}Cr_{0.105}MnGe_{1.05}$ melt-spun ribbons have been previously reported [12].

Fig. 2 shows the isofield $M(T)$ curves on heating and cooling in magnetic fields of 10mT and 5 T. At low temperatures, the ZFC and FCC

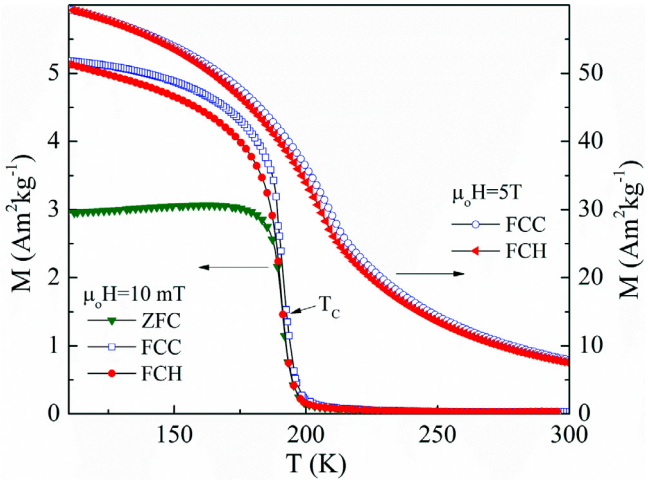

Fig. 2. Magnetization $M(T)$ curves of as-quenched $Ni_{0.895}Cr_{0.105}MnGe_{1.05}$ ribbons in applied magnetic fields of $\mu_o H$ = 10 mT (left Y-axis) and 5 T (right Y-axis).

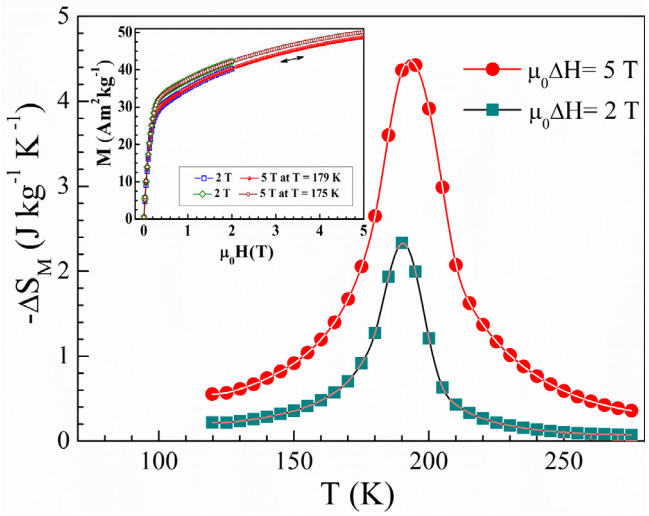

Fig. 3. Magnetic entropy change $\Delta S_M(T)$ curves of $Ni_{0.895}Cr_{0.105}MnGe_{1.05}$ ribbons for magnetic field changes of $\mu_o\Delta H = 2$ T and 5 T. Inset: magnetization isotherms measured during increasing and decreasing magnetic field near the SOT.

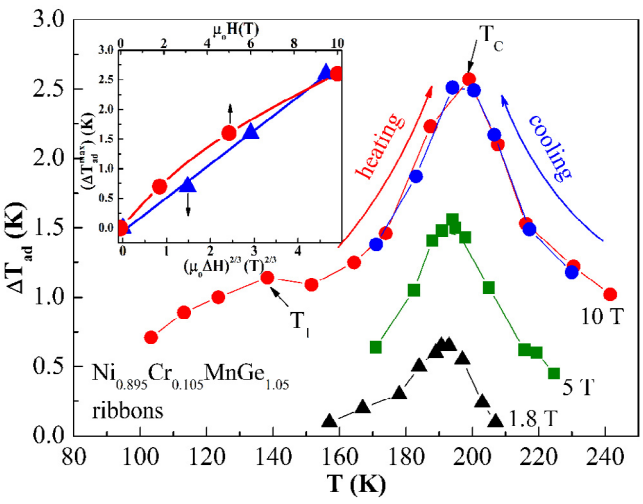

Fig. 4. $\Delta T_{ad}(T)$ curves measured by the direct method in magnetic field changes of 1.8 T, 5 T, and 10 T. Inset: ΔT_{ad}^{max} plotted as a function of μ_oH (horizontal top axis) and $(\mu_o\Delta H)^{2/3}$ (horizontal bottom axis).

$M(T)$ curves measured at $\mu_0H = 10$ mT show a typical FM behavior. With increasing temperature, an abrupt change in magnetization from a FM to a paramagnetic (PM) state was observed at the Curie temperature (T_C) ~192 K. The T_C was determined from the minimum of the dM/dT vs. T curve calculated from the magnetization curve during the heating cycle. The absence of thermal hysteresis in the heating and cooling $M(T)$ curves indicates the second order nature of the magnetic phase transition (SOT). Unlike the bulk $Ni_{0.895}Cr_{0.105}MnGe_{1.05}$ compound, which showed a first-order MST and a SOT, only a SOT was observed in the as-quenched ribbons. The $M(T)$ measurements at high field ($\mu_0H = 5$ T) showed similar behavior to those measured at low field with a broad transition shifted to ~210 K.

The magnetic entropy change (ΔS_M), across the SOT (Fig. 3) for magnetic field changes of $\mu_0\Delta H = 2$ and 5 T were calculated from the magnetization isotherms using the Maxwell relation $\Delta S_M(T) = \mu_0 \int_0^{\mu_0 H} \left(\frac{\partial M}{\partial T}\right)_{\mu_0 H} dH$. Normal (negative) ΔS_M peak values of -4.4 and -2.3 J kg^{-1} K^{-1} were observed at the SOT for field changes of 5 T and 2 T, respectively. Moreover, magnetization isotherms measured in the temperature range of the full-width at half-maximum (δT_{FWHM}) of the $\Delta S_M(T)$ curve near the SOT (see the inset of Fig. 3) were found to be fully reversible (i.e., no hysteresis loss), indicating a reversible MCE.

Fig. 4 shows the $\Delta T_{ad}(T)$ curves measured using the direct method in magnetic fields of 1.8 T, 5 T, and 10 T. The symmetric shape of the $\Delta T_{ad}(T)$ curves, which is characteristic of second-order magnetic phase transitions, is consistent with the $M(T)$ measurements (see Fig. 2). The peak positions of the $\Delta T_{ad}(T)$ curves shifted toward higher temperature, and the peak heights of the $\Delta T_{ad}(T)$ curves increased with increasing field. Positive values of ΔT_{ad} (i.e., heating) were observed, with a maximum value near the second order FM-PM transition. The maximum values of ΔT_{ad} near T_C were found to be 0.6, 1.6, and 2.6 K in magnetic field changes of 1.8 T, 5 T, and 10 T, respectively. Previous reports on ΔT_{ad} measurements in MnTX compounds showed that the ΔT_{ad} values (see Table 1) strongly depend on the samples thermomagnetic history (heating or cooling protocols) and strongly reduces due to (i) competition between structural and magnetic transitions [23], (ii) low field sensitivity of the phase transition [22], and (iii) large field dependence of the metamagnetic transition temperature at strong magnetic fields [24]. However, in $Ni_{0.895}Cr_{0.105}MnGe_{1.05}$ ribbons, we notice that the $\Delta T_{ad}(T)$ curves obtained during heating and cooling cycles coincided, indicating a reversible MCE in this system. A maximum ΔT_{ad} width of δT_{FWHM} ~61 K, defined as the full-width at half-maximum of the ΔT_{ad}(T) curve, was observed for $\mu_0H = 10$ T. The values of δT_{FWHM} at different magnetic field changes are given in Table 1. High reversibility and large widths of the MCE parameters are important preconditions for MCE applications.

An additional maximum of ~1 K was observed at $T_1 = 137$ K in the $\Delta T_{ad}(T)$ curves measured at 10 T. This maximum is most likely associated with some field-induced phase transition. A comparison between ΔT_{ad}^{max} values obtained in this system with those reported for other compounds belonging to MnTX family is given in Table 1.

In order to investigate the field change dependence of the adiabatic temperature change, ΔT_{ad}^{max} values at different magnetic fields $\mu_0\Delta H$ have been plotted (see inset of Fig. 4). The value of ΔT_{ad}^{max} increased nonlinearly with applied magnetic field. A non-saturating behavior of ΔT_{ad} was observed in magnetic fields up to 10 T, indicating an applied field of 10 T is not sufficient to fully saturate the FM phase in this system.

According to the mean field model, and Landau's thermodynamic theory of phase transitions, the magnetic field dependence of the maximum adiabatic temperature change in the vicinity of a SOT can be described by the power law, $\Delta T_{ad}^{max} \propto (\mu_o\Delta H)^{2/3}$ [29,30]. As shown in the inset of Fig. 4, a plot of ΔT_{ad}^{max} versus $(\mu_o\Delta H)^{2/3}$, and the fit of the data points to a straight line, verify that ΔT_{ad}^{max} is a linear function of $(\mu_o\Delta H)^{2/3}$ near T_C. These results further confirm that Landau's thermodynamic theory for SOTs is valid even for high magnetic fields up to 10 T in this system.

4. Conclusion

In conclusion, the MCE parameters, ΔS_M and ΔT_{ad}, in rapidly solidified $Ni_{0.895}Cr_{0.105}MnGe_{1.05}$ melt-spun ribbons were explored using direct and indirect measurements in magnetic field changes up to 10 T at the second order transition. The maximum values of the adiabatic temperature changes (ΔT_{ad}^{max}) and the magnetic entropy change ($|\Delta S_M^{peak}|$) near the Curie temperature (T_C) were found to be ~2.6 K ($\mu_o\Delta H = 10$ T) and 4.4 J kg^{-1} K^{-1} ($\mu_o\Delta H = 5$ T), respectively. Both ΔT_{ad} and the isothermal magnetization curves were found to be completely reversible, indicating that the MCE is reversible. The widths of the $\Delta T_{ad}(T)$ curves were found to increase with applied magnetic field with a maximum δT_{FWHM} of ~61 K at 10 T. A non-saturating behavior of ΔT_{ad}^{max} was observed even in high fields up to 10 T. The ΔT_{ad}^{max} obeyed the power law $\Delta T_{ad}^{max} \propto (\mu_o\Delta H)^{2/3}$ near the SOT. The ΔT_{ad} values obtained, together with previously reported values in similar

Table 1
A comparison of ΔT_{ad}^{max} measured for $Ni_{0.895}Cr_{0.105}MnGe_{1.05}$ ribbons with other compounds belonging to MnTX family. The full-width at half-maximum of the $\Delta T_{ad}(T)$ curves (δT_{FWHM}) at different applied magnetic fields for $Ni_{0.895}Cr_{0.105}MnGe_{1.05}$ ribbons are also given.

Alloys	ΔT_{ad} (K)	δT_{FWHM} (K)	Phase transition order	Reference
$Ni_{0.895}Cr_{0.105}MnGe_{1.05}$ (ribbons)	0.7 K at $\mu_0\Delta H$ = 1.8 T	30	SOT	this work
	1.6 K at $\mu_0\Delta H$ = 5 T	36		
	2.6 K at $\mu_0\Delta H$ = 10 T	61		
$Mn_{0.87}Fe_{0.13}NiGe$ (bulk)	0.5 K (cooling) at $\mu_0\Delta H$ = 1.93 T	–	FOT	[22]
$Mn_{0.7}Fe_{0.3}NiGe_{0.7}Si_{0.3}$ (bulk)	0.3 K (heating) at $\mu_0\Delta H$ = 1.93 T	–		
	1.3 K (cooling) at $\mu_0\Delta H$ = 1.93 T			
$MnCo_{0.95}Ge$ (bulk)	0.9 K at $\mu_0\Delta H$ = 1.9 T	–	SOT	[23]
$MnCo_{0.95}Ge_{0.95}$ (bulk)	1.5 K at $\mu_0\Delta H$ = 1.9 T	–	SOT	
$MnCo_{0.95}Ge_{0.97}$ (bulk)	0.3 K (heating) at $\mu_0\Delta H$ = 1.9 T	–	FOT	
	1.5 K (cooling) at $\mu_0\Delta H$ = 1.9 T			
CoMnSi	1.5 K at $\mu_0\Delta H$ = 5 T	–	FOT	[24]
$CoMnGe_{0.945}Ga_{0.055}$ (bulk)	6.5 K[#] at $\mu_0\Delta H$ = 2 T	–	FOT	[28]

[#] ΔT_{ad} from indirect measurement.

systems (Ni-Mn-Ge, Co-Mn-Si, and Mn-Co-Ge), show a relatively low ΔT_{ad}^{max}, which may affect the material's performance for MCE. However, the reversible magnetocaloric effect may also be interesting for practical application.

Acknowledgments

This work was supported by the U.S. Department of Energy (DOE), Office of Science, Basic Energy Sciences (BES) under Award No. DE-FG02-06ER46291 (SIU) and DE-FG02-13ER46946 (LSU). The work of Y. S. Koshkidko was supported by the National Science Center, Poland through the SONATA Program under Grant No. 2016/21/D/ST3/03435. J.L. Sánchez Llamazares acknowledges support from Laboratorio Nacional de Nanociencias y Nanotecnología (LINAN, IPICyT). C.F. Sánchez-Valdés is grateful to DMCU-UACJ for supporting his research stays at IPICyT (program PFCE and academic mobility grant); also, for the financial support received from PRODEP-SEP, Mexico (Grant No. UACJ-PTC-383).

References

[1] V.K. Pecharsky, K.A. Gschneidner Jr., Phys. Rev. Lett. 78 (1997) 4494–4497.
[2] O. Tegus, E. Bruck, K.H.J. Buschow, F.R. de Boer, Nature 415 (2002) 150–152.
[3] A. Fujita, S. Fujieda, Y. Hasegawa, K. Fukamichi, Phys. Rev. B 67 (2003) 104416.
[4] I. Dubenko, M. Khan, A.K. Pathak, B.R. Gautam, S. Stadler, N. Ali, J. Magn. Magn. Mater. 321 (2009) 754–757.
[5] H. Wada, Y. Tanabe, Appl. Phys. Lett. 79 (2001) 3302–3304.
[6] Z.B. Li, J.L. Sánchez Llamazares, C.F. Sánchez-Valdés, Y.D. Zhang, C. Esling, X. Zhao, L. Zuo, Appl. Phys. Lett. 100 (2012) 174102.
[7] K.A. Gschneidner Jr., V.K. Pecharsky, A.O. Tsokol, Rep. Prog. Phys. 68 (2005) 1479–1539.
[8] A.M. Tishin, Y.I. Spichkin, The Magnetocaloric Effect and its Applications, Institute of Physics (IOP), Bristol, 2003.
[9] W. Bazela, A. Szytuła, J. Todorović, Z. Tomkowicz, A. Zieba, Phys. Status Solidi A 38 (1976) 721–729.
[10] T. Kanomata, H. Ishigaki, T. Suzuki, H. Yoshida, S. Abe, T. Kaneko, J. Magn. Magn. Mater. 140–144 (1995) 131–132.
[11] A. Aryal, A. Quetz, S. Pandey, M. Eubank, T. Samanta, I. Dubenko, S. Stadler, N. Ali, J. Appl. Phys. 117 (2015) 17A711.
[12] A. Aryal, A. Quetz, C.F. Sánchez-Valdés, P.J. Ibarra-Gaytán, S. Pandey, I. Dubenko, J.L. Sánchez Llamazares, S. Stadler, N. Ali, Intermetallics 97 (2018) 89–94.
[13] A. Aryal, A. Quetz, S. Pandey, I. Dubenko, S. Stadler, N. Ali, Adv. Cond. Matt. Phys. 07 (2017) 1–6.
[14] A. Aryal, A. Quetz, S. Pandey, T. Samanta, I. Dubenko, M. Hill, D. Mazumdar, S. Stadler, N. Ali, J. Alloys Compd. 709 (2017) 142–146.
[15] A. Aryal, S. Pandey, I. Dubenko, D. Mazumdar, S. Stadler, N. Ali, MRS Commun. (2019), https://doi.org/10.1557/mrc.2018.228.
[16] T. Samanta, D.L. Lepkowski, A. Us Saleheen, A. Shankar, J. Prestigiacomo, I. Dubenko, A. Quetz, I.W.H. Oswald, G.T. McCandless, J.Y. Chan, P.W. Adams, D.P. Young, N. Ali, S. Stadler, Phys. Rev. B 91 (2015) 020401(R).
[17] T. Samanta, D.L. Lepkowski, A. Us Saleheen, A. Shankar, J. Prestigiacomo, I. Dubenko, A. Quetz, I.W.H. Oswald, G.T. McCandless, J.Y. Chan, P.W. Adams, D.P. Young, N. Ali, S. Stadler, J. Appl. Phys. 117 (2015) 123911.
[18] T. Samanta, P. Lloveras, A. Us Saleheen, D.L. Lepkowski, E. Kramer, I. Dubenko, P.W. Adams, D.P. Young, M. Barrio, J. Ll Tamarit, N. Ali, S. Stadler, Appl. Phys. Lett. 112 (2018) 021907.
[19] V. Franco, J.S. Blázquez, J.J. Ipus, J.Y. Law, L.M. Moreno-Ramírez, A. Conde, Prog. Mater. Sci. 93 (2018) 112–232.
[20] N.T. Trung, L. Zhang, L. Caron, K.H.J. Buschow, E. Bruck, Appl. Phys. Lett. 96 (2010) 172504.
[21] T. Samanta, I. Dubenko, A. Quetz, S. Stadler, N. Ali, Appl. Phys. Lett. 101 (2012) 242405.
[22] A. Taubel, T. Gottschall, M. Fries, T. Faske, K. Skokov, O. Gutfleisch, J. Phys. D: Appl. Phys. 50 (2017) 464005.
[23] J. Liu, K. Skokov, O. Gutfleisch, Scr. Mater. 66 (2012) 642–645.
[24] K.G. Sandeman, R. Daou, S. Ozcan, J.H. Durrell, N.D. Mathur, D.J. Fray, Phys. Rev. B 74 (2006) 224436.
[25] A. Quintana-Nedelcos, J.L. Sánchez Llamazares, C.F. Sánchez-Valdés, P. Álvarez Alonso, P. Gorria, P. Shamba, N.A. Morley, J. Alloys Compd. 694 (2017) 1189–1195.
[26] Y.S. Koshkid'ko, J. Ćwik, T.I. Ivanova, S.A. Nikitin, M. Miller, K. Rogacki, J. Magn. Magn. Mater. 433 (2017) 234–238.
[27] Powder Diffraction File, Alphabetical Indexes for experimental Patterns, Inorganic Phases, JCPDS International Center for Diffraction Data (2002), Newtown Square, Pennsylvania, U.S.A., ISSN 8756-0127.
[28] I. Dincer, E. Yüzüak, G. Durak, Y. Elerman, J. Alloys Compd. 588 (2014) 332–336.
[29] H. Oesterreicher, F.T. Parkar, J. Appl. Phys. 55 (1984) 4334–4338.
[30] K.P. Belov, Magnetic Transitions, Consultants Bureau (eds.), New York (1961).